

# Deep Eutectic Solvent Eutectogels for Delivery of Broad-Spectrum Antimicrobials

Z. L. Shaw, Miyah N. Awad, Soroosh Gharehgozlo, Tamar L. Greaves, Hanif Haidari, Zlatko Kopecki, Gary Bryant, Patrick T. Spicer, Sumeet Walia,\* Aaron Elbourne,\* and Saffron J. Bryant\*



Cite This: *ACS Appl. Bio Mater.* 2024, 7, 1429–1434



Read Online

ACCESS |



Metrics & More



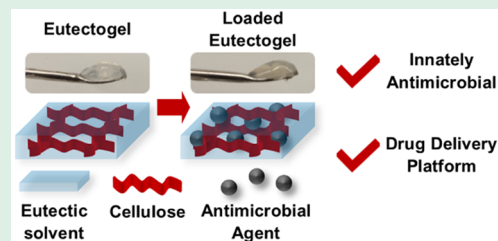
Article Recommendations



Supporting Information

**ABSTRACT:** Gel-based wound dressings have gained popularity within the healthcare industry for the prevention and treatment of bacterial and fungal infections. Gels based on deep eutectic solvents (DESs), known as eutectogels, provide a promising alternative to hydrogels as they are non-volatile and highly tunable and can solubilize therapeutic agents, including those insoluble in hydrogels. A choline chloride:glycerol-cellulose eutectogel was loaded with numerous antimicrobial agents including silver nanoparticles, black phosphorus nanoflakes, and commercially available pharmaceuticals (octenidine dihydrochloride, tetracycline hydrochloride, and fluconazole). The eutectogels caused >97% growth reduction in Gram-positive methicillin-resistant *Staphylococcus aureus* and Gram-negative *Pseudomonas aeruginosa* bacteria and the fungal species *Candida albicans*.

**KEYWORDS:** Deep eutectic solvent, eutectogel, gel, antimicrobial gel, antibacterial, antifungal



Antimicrobial resistant (AMR) pathogens are a developing global health threat, with approximately 6 million deaths/year associated with AMR bacterial infections,<sup>1,2</sup> while pathogenic fungal infections cause up to 1.5 million deaths/year, with higher mortality rates if treatment is delayed.<sup>3</sup> The cost of treating these infections is over USD\$20 billion each year<sup>4</sup> and could rise to USD\$1 trillion by 2050 with a concurrent rise to 10 million deaths/year.<sup>1</sup>

Antimicrobial gels are a popular treatment method for a range of wound environments, including minor cuts, burns, surgical implant sites, and chronic wounds.<sup>5,6</sup> Gels derived from natural polymers including chitosan, gelatin, and cellulose have high levels of biocompatibility and biodegradation<sup>7–9</sup> and can be loaded with antimicrobial agents such as antibiotics, antiseptics, or nanoparticles.<sup>9–12</sup> Hydrogels, which are water based, have gained popularity due to their flexibility, high viscosity, and ability to provide a moist environment that promotes wound healing.<sup>5,6</sup> However, many hydrogels readily dehydrate upon application, requiring regular replenishment, which is time consuming, painful for patients, can disrupt the healing process, and significantly increases the risk of localized infection.<sup>13</sup>

One possible solution is the use of “eutectogels”, gels based on deep eutectic solvents (DESs), rather than water.<sup>14,15</sup> DESs are a tailorable class of solvents that are composed of a hydrogen bond donor and a hydrogen bond acceptor that has a melting point much lower than either of the individual components.<sup>16</sup> These solvents are relatively cheap, nontoxic, biocompatible, and highly tailorable, leading to their interest for self-assembly, extraction, and cryopreservation, among

other applications.<sup>17–20</sup> DES-cellulose gels are highly tailorable, as both the DES composition and amount of cellulose used can alter the behavior of the gels.<sup>21</sup> Importantly, eutectogels provide a moist environment that will not dry out due to the non-volatile nature of the DES components.<sup>15</sup> They also provide a favorable environment for hydrophobic drugs or nanomaterials that are destabilized by water.<sup>15,22</sup>

Here, choline chloride:glycerol (ChCl-Gly)-cellulose eutectogels are used as a broad-spectrum antimicrobial delivery platform which can be applied to contaminated surfaces. ChCl-Gly was selected as the DES for this gel as it is inexpensive, biodegradable, and nontoxic.<sup>23,24</sup> The antimicrobial efficiency was tested against model Gram-positive methicillin-resistant *Staphylococcus aureus* (MRSA) and Gram-negative *Pseudomonas aeruginosa* (*P. aeruginosa*) bacterial cells, as well as the pathogenic fungal species *Candida albicans* (*C. albicans*). The eutectogel was loaded with known antimicrobial agents: two nanomaterial-based agents, 10 nm silver nanoparticles (AgNPs)<sup>12</sup> and 2D black phosphorus nanoflakes (BPNFs),<sup>25,26</sup> and three pharmaceutical agents, octenidine dihydrochloride (Oct),<sup>27</sup> tetracycline hydrochloride (Tetra),<sup>11,28</sup> and fluconazole (Fluc),<sup>29</sup> selected as commercially used antiseptic, antibiotic, and antifungal agents,

**Received:** October 18, 2023

**Revised:** February 22, 2024

**Accepted:** February 26, 2024

**Published:** March 6, 2024



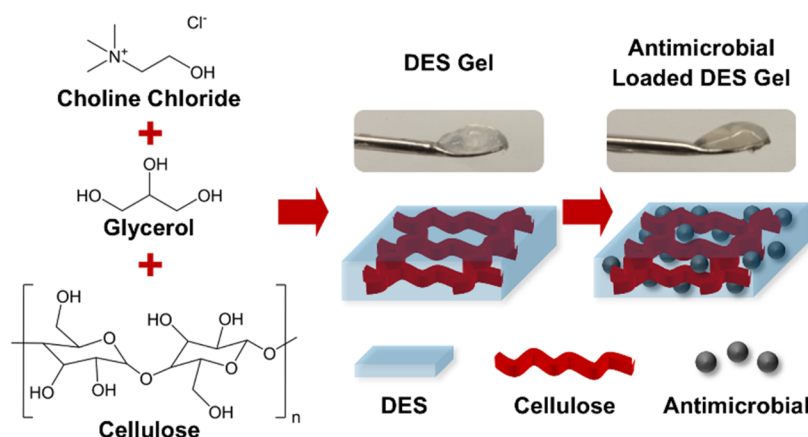


**Figure 1.** Composition of the eutectogel with and without antimicrobial agent.

respectively. Although there has been a recent increase in Tetra resistant bacterial infections, Tetra was selected as the representative antibiotic for this study, as the antibiotic response is well documented, and the bacterial strains used were not Tetra resistant.

The eutectogel synthesis and experimental details can be found in the [Supporting Information](#), and an overview of the eutectogel composition is shown in [Figure 1](#). Briefly, ChCl-Gly was mixed with a hydrated pellicle containing 0.8 wt % cellulose in a 1:1 weight ratio to form a “bare” gel. The antimicrobial agents (AgNPs, BPNFs, Oct, Tetra, or Fluc) were then added into the gels at the desired concentrations. The excess water was removed by freeze-drying the gels before characterization and antimicrobial testing. Images of the gels after drying are shown in [Figure S1](#).

The nanoparticles were visualized, and the size distribution was determined prior to loading into the eutectogels. Transmission electron microscopy (TEM) micrographs of the purchased AgNPs demonstrated an average diameter of  $10.1 \pm 1.8$  nm ([Figure S2](#)). For the prepared BPNFs, scanning electron micrographs and TEM were used for visualization ([Figure S3A, B](#)), while atomic force microscopy was used to determine the size distribution of the nanoflakes ([Figure S3C](#)). The BPNFs had an average flake thickness of  $38 \pm 23$  nm and length of  $237 \pm 112$  nm ([Figure S3D, E](#)).

Prior to addition of the antimicrobial agents, the bare eutectogel was imaged using differential interference contrast (DIC) microscopy ([Figure 2A](#)). The DIC image shows a crowded field of cellulose fibers hundreds of micrometers long with a thickness in the micrometer scale or smaller. The high aspect ratio of the cellulose fibers results in a highly efficient

network within the DES, providing the yield stress needed to adhere to skin and not flow under gravity. Bundling and star-like forms are also visible in the image, indicating the high degree of entanglement of the fibers and their highly flexible nature that enables an easy transition to flowability from the gel state under applied shear stresses. The shear-thinning behavior of the bare eutectogel is consistent with previous reports on similar systems<sup>15</sup> and is retained upon addition of the antimicrobial agents ([Figure 2B](#)). This behavior is critical for wound-dressing applications as it relates to how easy it is to apply to the skin-like moisturizers and lotion and how well the gel will stay in place once applied. The addition of the antimicrobials affected the absolute values of the viscosity. However, this may be due to unequal water absorption between the samples as DESs are known to rapidly absorb atmospheric water, and this can have a significant effect on their viscosity.<sup>30</sup> Fourier transform infrared (FTIR) spectroscopy was used to provide insight into the chemical structure of the gel. The average absorbance spectra for all the gels with antimicrobials present are given in [Figure S4](#) and show no significant peak shifts when compared to the bare gel, indicating that the antimicrobial agents did not cause any major chemical changes to the eutectogel. The specific fibril arrangements and interactions with DESs are beyond the scope of this paper but will be explored in the future.

The antimicrobial properties of the eutectogels were assessed against three model pathogenic species, MRSA, *P. aeruginosa*, and *C. albicans*, which are commonly encountered in infected wounds.<sup>2,3</sup> Initially, the antimicrobial ability of the bare eutectogel was determined by using broth dilution assays ([Figure 3A](#)) to determine the concentration of colony forming units (CFU/mL) in the sample after exposure. Notably, all microbial species had a  $>1.0 \log_{10}$  reduction ( $>90\%$  reduction) ([Figure 3C](#) and [Table 1](#)) after 24 h of exposure compared to a sample treated with phosphate buffer solution (PBS), suggesting the bare eutectogel possesses some antimicrobial properties. To explore this further, antimicrobial activity was tested using zone of inhibition (ZOI) assays ([Figure 3B](#)), and the reported values are the measured ZOI diameter minus the well diameter ([Figure 3D](#)). Unlike the dilution test described above, the bare gel showed little-to-no growth inhibition, with all three pathogenic species having a ZOI of  $0.6 \pm 0.5$  mm. This is consistent with previous studies of ChCl-Gly which showed no ZOI for *Staphylococcus aureus*, *Listeria monocytogenes*, *Escherichia coli*, or *Salmonella enteritidis*.<sup>31</sup> The average CFU/mL reduction and ZOI measurements are

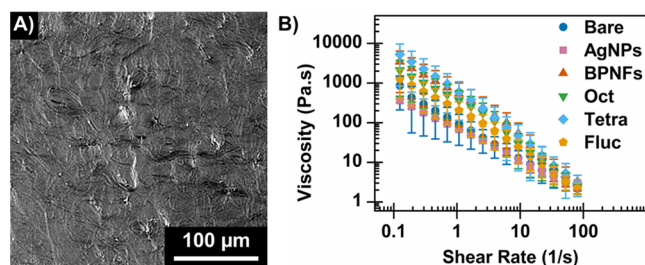


**Figure 2.** (A) DIC image of the bare eutectogel. (B) Viscosity as a function of shear rate for the eutectogels. Experiments were performed in duplicate, and the mean  $\pm$  the difference is shown.

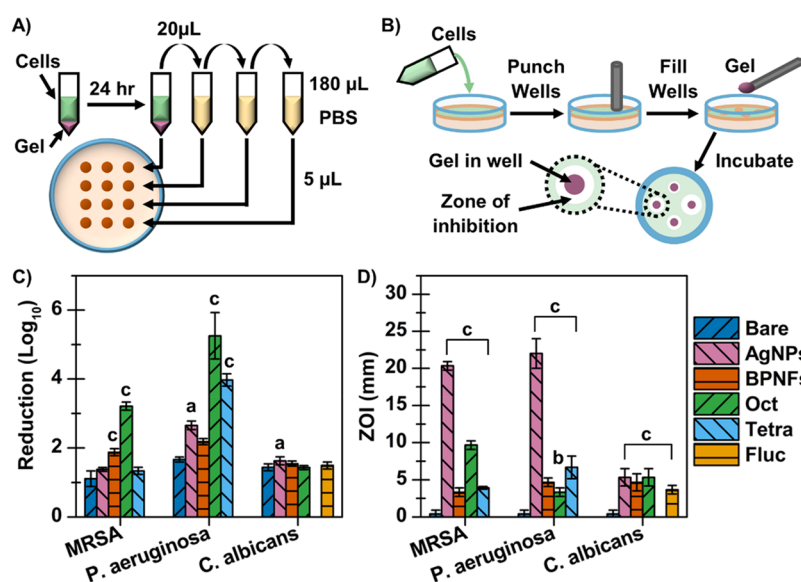


**Figure 3.** Overview of the (A) colony counting/broth dilution and (B) ZOI protocol used. (C) Reduction in cell count for the bare and antimicrobial-loaded gels as a  $\log_{10}$  reduction of the control after 24 h exposure. (D) ZOI diameters for the eutectogels. The mean  $\pm$  SD values of four measurements are shown. Tetra is an antibacterial and so was only tested against MRSA and *P. aeruginosa*, while Fluc is an antifungal and so was only tested against *C. albicans*. The significance of differences compared to the bare gel was determined using ANOVA one-way analysis followed by Tukey's multiple comparison test. a =  $P < 0.01$ , b =  $P < 0.001$ , and c =  $P < 0.0001$ ; all data points within the horizontal bracket have the same P value unless otherwise labeled.

**Table 1. Summary of Antimicrobial Activity of Bare and Antimicrobial-Loaded Gels<sup>a</sup>**

	MRSA		<i>P. aeruginosa</i>		<i>C. albicans</i>	
	Reduction ( $\log_{10}$ )	ZOI (mm)	Reduction ( $\log_{10}$ )	ZOI (mm)	Reduction ( $\log_{10}$ )	ZOI (mm)
Bare	1.1 $\pm$ 0.2	0.6 $\pm$ 0.5	1.7 $\pm$ 0.1	0.6 $\pm$ 0.5	1.4 $\pm$ 0.1	0.6 $\pm$ 0.5
AgNPs	1.4 $\pm$ 0.1	20.0 $\pm$ 0.1	2.7 $\pm$ 0.1	22 $\pm$ 2	1.6 $\pm$ 0.1	5.0 $\pm$ 1
BPNFs	1.9 $\pm$ 0.1	3.3 $\pm$ 0.6	2.2 $\pm$ 0.1	4.7 $\pm$ 0.6	1.5 $\pm$ 0.1	5.0 $\pm$ 1
Oct	3.2 $\pm$ 0.1	9.7 $\pm$ 0.6	5.3 $\pm$ 0.7	3.0 $\pm$ 1	1.4 $\pm$ 0.1	5.0 $\pm$ 0.1
Tetra	1.3 $\pm$ 0.1	10.7 $\pm$ 0.6	4.0 $\pm$ 0.2	7.0 $\pm$ 2		
Fluc					1.5 $\pm$ 0.1	3.7 $\pm$ 0.6

<sup>a</sup>Data reported as mean  $\pm$  standard deviation calculated from four measurements,  $n = 4$ .

summarized in Figure 3C and D and Table 1. Representative images of the agar plates used for ZOI measurements are shown in Figure S5.

The differences in antimicrobial response between these dilution assays and ZOI values has been observed previously<sup>31,32</sup> and is likely because the DESs create an osmotic imbalance which dehydrates the microbes in the broth dilution assay. By contrast, the highly viscous eutectogel and agar in the ZOI tests limit diffusion, and the bare eutectogel has no effect on bacterial growth.<sup>32</sup>

The addition of antimicrobial agents generally increased the antimicrobial activity compared with the results for the bare gels (Figure 3C, D and Table 1). For each antimicrobial agent, initial concentration studies were conducted, and the loaded eutectogels all showed a concentration-dependent antimicrobial response, with higher concentrations showing the strongest antimicrobial response (Figures S6–10 and Tables S1–5). To compare the loaded gels with the bare eutectogel, one loading concentration was selected for each antimicrobial, and the selection criteria can be found in the concentration study section of the Supporting Information. The concentrations selected for comparison were 20  $\mu\text{g/g}$  for AgNPs, 2.5 mg/g for BPNFs, 10  $\mu\text{g/g}$  for Oct, and 100  $\mu\text{g/g}$  for both Tetra and Fluc. The eutectogels successfully acted as a delivery

vehicle for all five of the antimicrobial agents against all three pathogenic species, demonstrating the versatility of this delivery vehicle.

For MRSA, the bare gel caused >90% reduction in live cells, and the addition of AgNPs or Tetra saw a small increase in the antimicrobial activity (Figure 3C). Previous work has explored the addition of Tetra into chitosan-based gels and reported similarly high antimicrobial ability against *S. aureus* and *E. coli*.<sup>8,11</sup> For Tetra to damage microbial cells, the compound needs to be taken up by the cell,<sup>28</sup> indicating that the larger drug molecule can diffuse through the eutectogel. Addition of BPNFs caused a significant increase in antimicrobial activity (>98% reduction) against MRSA. Previous work has reported a high antimicrobial response from lower concentrations of BPNFs in solution (>99% reduction of *S. aureus* with 100–1280  $\mu\text{g/mL}$ )<sup>26,33</sup> or modified BPNFs in a gelatin-based hydrogel (50  $\mu\text{g/mL}$  for a > 95% reduction in *S. aureus*).<sup>7</sup> However, when BPNFs are encapsulated or loaded into other gel environments, near-infrared (NIR) irradiation (5–10 min of 808 nm) is often required to induce the antimicrobial effect.<sup>7,34</sup> Under NIR irradiation, the temperature of BPNFs can increase to >50  $^{\circ}\text{C}$ , which can damage cell membranes.<sup>7</sup> In contrast, our BPNF-loaded eutectogel achieved a high antimicrobial response with only ambient light, as the reactive

oxygen species (ROS) produced by the BPNFs were able to diffuse through the eutectogel.<sup>25,26</sup> Similarly, the Oct-loaded eutectogel caused a >99.9% reduction in MRSA which is better than previously reported when loaded into a thermoresponsive copolymer gel, which required heat activation.<sup>27</sup>

In contrast, the ZOI tests showed no activity for the bare gel against MRSA and a significant increase in the ZOI with the addition of all five of the antimicrobials tested (Figure 3D). AgNPs resulted in the biggest ZOI (>20 mm), larger than previously reported for AgNP-loaded pluronic hydrogels.<sup>10</sup> This improved response may be linked to the greater relative diffusion of Ag<sup>+</sup> ions in our eutectogel compared with the AgNPs-pluronic gel, which could be aided by the lower viscosity. The ZOI around Oct-loaded gels was achieved at a much lower concentration than previously reported for a solution.<sup>9</sup>

*P. aeruginosa* had a similar response to MRSA. In the broth-dilution assay, the bare gel had some antimicrobial activity which was significantly increased on addition of the antimicrobial agents (Figure 3C). The 97% reduction for AgNP-loaded eutectogel is comparable to previously reported AgNP-pluronic hydrogels with similar AgNP concentrations.<sup>10</sup> As with MRSA, the >99.9% reduction achieved here with Oct-loaded gels is greater than the response reported for a copolymer gel.<sup>27</sup> Further, the ZOI of the loaded gels (Figure 3D) was significantly larger than that of the bare gel, and AgNPs resulted in the biggest ZOI. As seen with MRSA, both the AgNP- and Oct-loaded eutectogels showed better inhibition compared to previously reported hydrogels.<sup>9,10</sup>

Unlike bacteria, *C. albicans* had almost no significant difference between the bare and loaded eutectogels in the broth-dilution assay (Figure 3C), even when the concentration of the antifungal Fluc was increased from 0.1 to 1 mg/g (Figure S10A and Table S5). This suggests that the antimicrobial effect of the eutectogel on *C. albicans* is independent of the loaded antimicrobial agents. One possible reason could be the differences in the cell wall structure between bacterial and fungal cells. While bacterial cell walls are predominantly peptidoglycan, polysaccharides, and phospholipids, fungal cell walls are primarily composed of  $\beta$ -glucans, chitin, and glycoproteins.<sup>35</sup> These findings suggest that the eutectogel may interact with the components in the *C. albicans* cell wall, blocking the uptake of both nutrients and antimicrobial agents. The blocked uptake could result in cell death due to starvation, rather than the mechanisms of the antimicrobial agents, when the eutectogel is in direct contact with the fungal cells. However, further investigation into this interaction with other cell wall structures is still needed.

As with the bacteria, *C. albicans* also had a significantly greater ZOI for the loaded gels compared to that of bare eutectogels (Figure 3D). These ZOIs are smaller than previously reported for a 0.5% Oct solution,<sup>9</sup> likely due to the solution allowing for greater antimicrobial diffusion compared to gels. The Fluc-loaded eutectogel had a smaller ZOI compared to previously reported Fluc-loaded Carbopol hydrogels.<sup>29</sup> However, the hydrogels were loaded with propylene glycol-coated fluconazole nanoparticles,<sup>29</sup> and the specific concentration of Fluc is unclear, which makes direct comparison difficult.

The antibiofilm properties were further explored by exposing MRSA biofilms to bare and loaded eutectogels. After an additional 24 h of exposure, confocal laser scanning microscopy (CLSM) was used to determine the percentage

of dead cells and associated reduction of live cells in treated biofilms compared to untreated, along with changes in the biofilm thicknesses (Figure 4 and Table S6). Compared to the

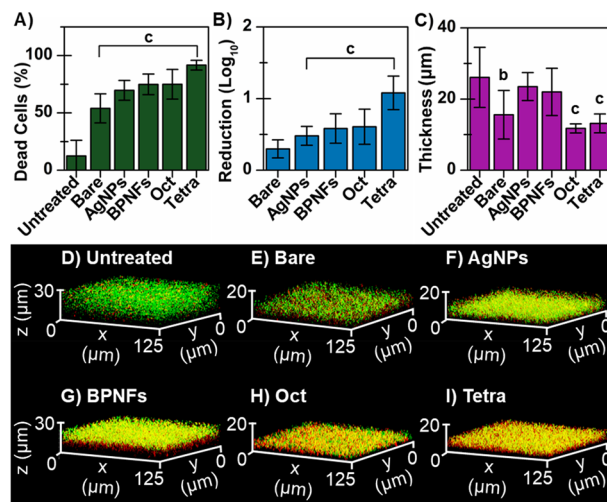


**Figure 4.** (A) Percentage of dead cells present. (B) Reduction in the percentage of living cells compared to an untreated biofilm. (C) Thickness of a MRSA biofilm after 24 h of exposure to the bare and loaded eutectogels. Each data point represents the mean  $\pm$  SD values. The significance compared to the untreated biofilm was determined using ANOVA one-way analysis followed by Tukey's multiple comparison test, b =  $P < 0.001$  and c =  $P < 0.0001$ . Representative 3D CLSM images for the (D) untreated biofilm, as well as biofilms exposed to (E) bare and (F) AgNPs-, (G) BPNFs-, (H) Oct-, and (I) Tetra-loaded eutectogels.

untreated biofilms (12% dead), all of the eutectogels caused a significant increase in cell death. The bare eutectogel led to 54% death, while the AgNPs-, BPNFs-, and Oct-loaded gels led to 70%–75% cell death, and the Tetra-loaded eutectogel achieved over 90% cell death. Although the reduction in living cells is lower for the biofilms than for the suspended MRSA cells (Table 1), the eutectogels were still able to effectively deliver the antimicrobial agents into the protective biofilm environment. Further, the overall thickness of the treated biofilms also decreased after exposure. The bare, Oct- and Tetra-treated biofilms were approximately half the thickness compared with the untreated biofilm. Representative 3D CLSM scans of the untreated and eutectogel-treated biofilms can be seen in Figure 4D–I. The significant reduction in both live cells and biofilm thickness further demonstrates the promising antimicrobial properties of the eutectogels and their potential as an effective drug delivery platform to aid in the treatment of surface wounds.

Eutectogels with and without antimicrobials demonstrated promising antimicrobial efficiency against model Gram-positive and Gram-negative bacterial cells as well as a pathogenic fungal species. The increased antimicrobial activity for the loaded eutectogels demonstrates the eutectogel's potential as an effective delivery platform for a range of antimicrobial compounds, including nanoparticle-based therapeutics and conventional pharmaceutical treatments. The eutectogel did not inhibit the varying antimicrobial mechanisms of the selected agents and allowed for the release and diffusion of both ions and larger drug molecules. This study has demonstrated for the first time the effectiveness of eutectogels as a broad-spectrum antimicrobial delivery platform. Eutecto-

gels have the potential to be an entirely new, versatile platform for treatment of AMR-related infections.

## ■ ASSOCIATED CONTENT

### SI Supporting Information

The Supporting Information is available free of charge at <https://pubs.acs.org/doi/10.1021/acsabm.3c00971>.

Material and methods section, image of bare and loaded eutectogels, size distribution of AgNPs and BPNFs, FTIR spectra of eutectogels, images of eutectogel ZOI, concentration study for loaded eutectogels, and MRSA biofilm results (PDF)

## ■ AUTHOR INFORMATION

### Corresponding Authors

**Sumeet Walia** – School of Engineering, RMIT University, Melbourne, VIC 3000, Australia; [orcid.org/0000-0002-3645-9847](https://orcid.org/0000-0002-3645-9847); Email: [sumeet.walia@rmit.edu.au](mailto:sumeet.walia@rmit.edu.au)

**Aaron Elbourne** – School of Science, RMIT University, Melbourne, VIC 3000, Australia; [orcid.org/0000-0002-4472-4372](https://orcid.org/0000-0002-4472-4372); Email: [aaron.elbourne@rmit.edu.au](mailto:aaron.elbourne@rmit.edu.au)

**Saffron J. Bryant** – School of Science, RMIT University, Melbourne, VIC 3000, Australia; [orcid.org/0000-0002-7202-3004](https://orcid.org/0000-0002-7202-3004); Email: [saffron.bryant@rmit.edu.au](mailto:saffron.bryant@rmit.edu.au)

### Authors

**Z. L. Shaw** – School of Engineering, RMIT University, Melbourne, VIC 3000, Australia

**Miyah N. Awad** – School of Science, RMIT University, Melbourne, VIC 3000, Australia; [orcid.org/0000-0001-8630-9444](https://orcid.org/0000-0001-8630-9444)

**Soroosh Gharehgozlo** – School of Science, RMIT University, Melbourne, VIC 3000, Australia

**Tamar L. Greaves** – School of Science, RMIT University, Melbourne, VIC 3000, Australia; [orcid.org/0000-0002-0298-0183](https://orcid.org/0000-0002-0298-0183)

**Hanif Haidari** – Future Industries Institute, University of South Australia, Mawson Lakes, South Australia 5095, Australia; [orcid.org/0000-0003-0189-7684](https://orcid.org/0000-0003-0189-7684)

**Zlatko Kopecki** – Future Industries Institute, University of South Australia, Mawson Lakes, South Australia 5095, Australia

**Gary Bryant** – School of Science, RMIT University, Melbourne, VIC 3000, Australia; [orcid.org/0000-0001-5483-7592](https://orcid.org/0000-0001-5483-7592)

**Patrick T. Spicer** – School of Chemical Engineering, University of New South Wales, Sydney 2052, Australia; [orcid.org/0000-0002-8562-3906](https://orcid.org/0000-0002-8562-3906)

Complete contact information is available at: <https://pubs.acs.org/doi/10.1021/acsabm.3c00971>

### Author Contributions

The manuscript was written through contributions of all authors. All authors have given approval to the final version of the manuscript.

### Notes

The authors declare no competing financial interest.

## ■ ACKNOWLEDGMENTS

A.E. is supported by an Australian Research Council (ARC) Discovery Early Career Research Award (DECRA) (DE220100511). Z.K. is supported by the Channel 7 Children's Research Foundation Fellowship. Z.L.S. acknowl-

edges this research was supported by an AINSE Ltd. Postgraduate Research Award (PGRA: ALNSTU13134). This work was partially funded by ARC DP220100020 (S.W.). The authors acknowledge the facilities and the scientific and technical assistance of the RMIT Microscopy & Microanalysis Research Facility (RMMF) and the RMIT Micro Nano Research Facility (MNRF) in the Victorian Node of the Australian National Fabrication Facility (ANFF).

## ■ REFERENCES

- (1) Humphreys, G.; Fleck, F. United Nations meeting on antimicrobial resistance: world leaders gather at the United Nations general assembly in New York this month to mount a response to the growing threat of antimicrobial resistance. In *Bulletin of the World Health Organization* **2016**, *94*, 638.
- (2) Boucher, H. W.; Talbot, G. H.; Bradley, J. S.; Edwards, J. E.; Gilbert, D.; Rice, L. B.; Scheld, M.; Spellberg, B.; Bartlett, J. Bad bugs, no drugs: no ESKAPE! An update from the infectious diseases society of America. *Clin. Infect. Dis.* **2009**, *48* (1), 1–12.
- (3) Boyce, K.; Morrissey, O.; Idnurm, A.; Macreadie, I. Insights into the global emergence of antifungal drug resistance. *Microbiol Aust* **2019**, *40* (2), 87.
- (4) Wozniak, T. M.; Dyda, A.; Merlo, G.; Hall, L. Disease burden, associated mortality and economic impact of antimicrobial resistant infections in Australia. *Lancet Reg Health - West Pac* **2022**, *27*, 100521.
- (5) Kopecki, Z. Development of next-generation antimicrobial hydrogel dressing to combat burn wound infection. *Biosci Rep* **2021**, *41* (2), BSR20203404.
- (6) Berthet, M.; Gauthier, Y.; Lacroix, C.; Verrier, B.; Monge, C. Nanoparticle-based dressing: the future of wound treatment? *Trends Biotechnol* **2017**, *35* (8), 770–784.
- (7) Ding, Q.; Sun, T.; Su, W.; Jing, X.; Ye, B.; Su, Y.; Zeng, L.; Qu, Y.; Yang, X.; Wu, Y. Bioinspired multifunctional black phosphorus hydrogel with antibacterial and antioxidant properties: a stepwise countermeasure for diabetic skin wound healing. *Adv. Healthcare Mater.* **2022**, *11* (12), 2102791.
- (8) Chen, H.; Xing, X.; Tan, H.; Jia, Y.; Zhou, T.; Chen, Y.; Ling, Z.; Hu, X. Covalently antibacterial alginate-chitosan hydrogel dressing integrated gelatin microspheres containing tetracycline hydrochloride for wound healing. *Mater. Sci. Eng., C* **2017**, *70*, 287–295.
- (9) Dydak, K.; Junka, A.; Dydak, A.; Brożyna, M.; Paleczny, J.; Fijalkowski, K.; Kubielas, G.; Aniolek, O.; Bartoszewicz, M. *In vitro* efficacy of bacterial cellulose dressings chemisorbed with antiseptics against biofilm formed by pathogens isolated from chronic wounds. *Int. J. Mol. Sci.* **2021**, *22* (8), 3996–3996.
- (10) Haidari, H.; Kopecki, Z.; Bright, R.; Cowin, A. J.; Garg, S.; Goswami, N.; Vasilev, K. Ultrasmall AgNP-impregnated biocompatible hydrogel with highly effective biofilm elimination properties. *ACS Appl. Mater. Interfaces* **2020**, *12* (37), 41011–41025.
- (11) Chen, H.; Li, B.; Feng, B.; Wang, H.; Yuan, H.; Xu, Z. Tetracycline hydrochloride loaded citric acid functionalized chitosan hydrogel for wound healing. *RSC Adv.* **2019**, *9* (34), 19523–19530.
- (12) Zakia, M.; Koo, J. M.; Kim, D.; Ji, K.; Huh, P.; Yoon, J.; Yoo, S. I. Development of silver nanoparticle-based hydrogel composites for antimicrobial activity. *Green Chem. Lett. Rev.* **2020**, *13* (1), 34–40.
- (13) An, H.; Zhang, M.; Zhou, L.; Huang, Z.; Duan, Y.; Wang, C.; Gu, Z.; Zhang, P.; Wen, Y. Anti-dehydration and rapid trigger-detachable multifunctional hydrogels promote scarless therapeutics of deep burn. *Adv. Funct. Mater.* **2023**, *33* (17), 2211182.
- (14) Zdanowicz, M.; Staciwa, P.; Jędrzejewski, R.; Szychaj, T. Sugar alcohol-based deep eutectic solvents as potato starch plasticizers. *Polymers* **2019**, *11* (9), 1385–1385.
- (15) Bryant, S. J.; da Silva, M. A.; Hossain, K. M. Z.; Calabrese, V.; Scott, J. L.; Edler, K. J. Non-volatile conductive gels made from deep eutectic solvents and oxidised cellulose nanofibrils. *Nanoscale Adv.* **2021**, *3* (8), 2252–2260.
- (16) Bryant, S. J.; Christofferson, A. J.; Greaves, T. L.; McConville, C. F.; Bryant, G.; Elbourne, A. Bulk and interfacial nanostructure and

properties in deep eutectic solvents: current perspectives and future directions. *JCIS* **2022**, *608*, 2430–2454.

(17) Bryant, S. J.; Bathke, E. K.; Edler, K. J. Bottom-up cubosome synthesis without organic solvents. *JCIS* **2021**, *601*, 98–105.

(18) de Almeida Pontes, P. V.; Ayumi Shiwaku, I.; Maximo, G. J.; Caldas Batista, E. A. Choline chloride-based deep eutectic solvents as potential solvent for extraction of phenolic compounds from olive leaves: extraction optimization and solvent characterization. *Food Chem.* **2021**, *352*, 129346–129346.

(19) Bryant, S. J.; Awad, M. N.; Elbourne, A.; Christofferson, A. J.; Martin, A. V.; Meftahi, N.; Drummond, C. J.; Greaves, T. L.; Bryant, G. Deep eutectic solvents as cryoprotective agents for mammalian cells. *J. Mater. Chem. B* **2022**, *10* (24), 4546–4560.

(20) Castro, V. I. B.; Craveiro, R.; Silva, J. M.; Reis, R. L.; Paiva, A.; Duarte, A. R. C. Natural deep eutectic systems as alternative nontoxic cryoprotective agents. *Cryobiology* **2018**, *83*, 15–26.

(21) Solomon, M. J.; Spicer, P. T. Microstructural regimes of colloidal rod suspensions, gels, and glasses. *Soft Matter* **2010**, *6* (7), 1391–1400.

(22) Kumar, M.; Shanthi, N.; Mahato, A. K.; Soni, S.; Rajnikanth, P. S. Preparation of luliconazole nanocrystals loaded hydrogel for improvement of dissolution and antifungal activity. *Heliyon* **2019**, *5* (5), e01688.

(23) Radošević, K.; Cvjetko Bubalo, M.; Gaurina Srček, V.; Grgas, D.; Landeka Dragičević, T.; Radojčić Redovniković, I. Evaluation of toxicity and biodegradability of choline chloride based deep eutectic solvents. *Ecotoxicol. Environ. Saf.* **2015**, *112*, 46–53.

(24) Chen, J.; Wang, Q.; Liu, M.; Zhang, L. The effect of deep eutectic solvent on the pharmacokinetics of salvianolic acid B in rats and its acute toxicity test. *J. Chromatogr. B* **2017**, *1063*, 60–66.

(25) Shaw, Z. L.; Kuriakose, S.; Cheeseman, S.; Mayes, E. L. H.; Murali, A.; Oo, Z. Y.; Ahmed, T.; Tran, N.; Boyce, K.; Chapman, J.; McConville, C. F.; Crawford, R. J.; Taylor, P. D.; Christofferson, A. J.; Truong, V. K.; Spencer, M. J. S.; Elbourne, A.; Walia, S. Broad-spectrum solvent-free layered black phosphorus as a rapid action antimicrobial. *ACS Appl. Mater. Interfaces* **2021**, *13* (15), 17340–17352.

(26) Virgo, E. P.; Haidari, H.; Shaw, Z. L.; Huang, L. Z. Y.; Kennewell, T. L.; Smith, L.; Ahmed, T.; Bryant, S. J.; Howarth, G. S.; Walia, S.; Cowin, A. J.; Elbourne, A.; Kopecki, Z. Layered black phosphorus nanoflakes reduce bacterial burden and enhance healing of murine infected wounds. *Adv. Ther.* **2023**, *6*, No. 2300235.

(27) Pan, F.; Zhang, S.; Altenried, S.; Zuber, F.; Chen, Q.; Ren, Q. Advanced antifouling and antibacterial hydrogels enabled by controlled thermo-responses of a biocompatible polymer composite. *Biomater. Sci.* **2022**, *10* (21), 6146–6159.

(28) Chopra, I.; Roberts, M. Tetracycline antibiotics: mode of action, applications, molecular biology, and epidemiology of bacterial resistance. *Microbiol. Mol. Biol. Rev.* **2001**, *65* (2), 232–260.

(29) Abdellatif, A. A. H.; El-Telbany, D. F. A.; Zayed, G.; Al-Sawahli, M. M. Hydrogel containing PEG-coated fluconazole nanoparticles with enhanced solubility and antifungal activity. *J. Pharm. Sci. Innovation* **2019**, *14* (2), 112–122.

(30) Meng, X.; Ballerat-Busserolles, K.; Husson, P.; Andanson, J.-M. Impact of water on the melting temperature of urea + choline chloride deep eutectic solvent. *New J. Chem.* **2016**, *40* (5), 4492–4499.

(31) Zhao, B.-Y.; Xu, P.; Yang, F.-X.; Wu, H.; Zong, M.-H.; Lou, W.-Y. Biocompatible deep eutectic solvents based on choline chloride: characterization and application to the extraction of rutin from *Sophora japonica*. *ACS Sustainable Chem. Eng.* **2015**, *3* (11), 2746–2755.

(32) Marchel, M.; Cieśliński, H.; Boczkaj, G. Deep eutectic solvents microbial toxicity: current state of art and critical evaluation of testing methods. *J. Hazard. Mater.* **2022**, *425*, 127963–127963.

(33) Sun, Z.; Zhang, Y.; Yu, H.; Yan, C.; Liu, Y.; Hong, S.; Tao, H.; Robertson, A. W.; Wang, Z.; Pádua, A. A. New solvent-stabilized few-layer black phosphorus for antibacterial applications. *Nanoscale* **2018**, *10* (26), 12543–12553.

(34) Huang, S.; Xu, S.; Hu, Y.; Zhao, X.; Chang, L.; Chen, Z.; Mei, X. Preparation of NIR-responsive, ROS-generating and antibacterial black phosphorus quantum dots for promoting the MRSA-infected wound healing in diabetic rats. *Acta Biomaterialia* **2022**, *137*, 199–217.

(35) Ghassemi, N.; Poulhazan, A.; Deligey, F.; Mentink-Vigier, F.; Marcotte, I.; Wang, T. Solid-state NMR investigations of extracellular matrixes and cell walls of algae, bacteria, fungi, and plants. *Chem. Rev.* **2022**, *122* (10), 10036–10086.